Corrosion protection mechanism of Ce 3+ /polyethylene glycol systems inhibitors for mild steel in sulfate solution

Article *in* Materials and Corrosion · February 2023

DOI: 10.1002/maco.202313727

CITATIONS
0

READS
88

4 authors, including:

Hichem Boudellioua
Université Amar Telidji Laghouat
5 PUBLICATIONS **97** CITATIONS

SEE PROFILE

Youcef Hamlaoui
Université de Souk Ahras
17 PUBLICATIONS **554** CITATIONS

SEE PROFILE

F. Pedraza
La Rochelle Université
153 PUBLICATIONS **2,707** CITATIONS

SEE PROFILE

Received: 6 January 2023 | Accepted: 30 January 2023

DOI: 10.1002/maco.202313727

ARTICLE

Materials and Corrosion

Corrosion protection mechanism of Ce^{3+}/polyethylene glycol systems inhibitors for mild steel in sulfate solution

Hichem Boudellioua[1,2] | **Youcef Hamlaoui**[2] | **Lakhdar Tifouti**[3] | **Fernando Pedraza**[4]

[1]Laboratoire de Génie des Procédés, Université Amar Telidji, Laghouat, Algérie

[2]Laboratoire de Physique de la Matière et Rayonnement (LPMR), Faculté des Sciences et de Technologie, Université Mohamed Chérif Messaadia, Souk-Ahras, Algérie

[3]Laboratoire de Génie de l'Environnement (LGE), Université Badji Mokhtar, El Hadjar-Annaba, Algérie

[4]Laboratoire des Sciences de l'Ingénieur pour l'Environnement (LaSIE, UMR-CNRS 7356), Université de La Rochelle, Avenue Michel Crépeau, La Rochelle, France

Correspondence
Hichem Boudellioua, Laboratoire de Génie des Procédés, Université Amar Telidji, BP G37, Laghouat 03000, Algérie.
Email: hichem_boudellioua@yahoo.fr

Abstract

In the present paper, cerium nitrate salt was used as a green inhibitor to improve the corrosion resistance of mild steel in 0.1 M Na_2SO_4 solution. To increase the barrier effect and film stability of the protective layer, polyethylene glycol (PEG) was added. The corrosion tests were evaluated using d.c polarization techniques and electrochemical impedance spectroscopy. The composition and morphology of the sample surface were characterized using Raman spectroscopy and MEB/EDS analysis. The results show that the presence of PEG improved relatively the corrosion resistance of mild steel due to the removal of cracks, the pores blocking the formed film and the enhancement of adhesion and compactness of the cerium-based film. Consequently, the protective film became more coherent on the steel surface. Furthermore, the potentiodynamic polarization indicated that the Ce^{3+}/PEG system behaved as a mixed-type inhibitor with the dominant effect of the cathodic part.

KEYWORDS

corrosion inhibition, electrochemical approach, mild steel, organic/inorganic complex, surface analysis

1 | INTRODUCTION

The availability, high machinability, relatively inexpensive, and excellent mechanical properties of mild steel make it a popular choice for a wide range of applications, including chemical and petrochemical industries.[1] However, one major problem of these industries is their degradation caused by corrosion that needs to be reduced to extend the lifetime of steel. Mild steel can be protected against corrosion by deposit coatings in a variety of ways, including the following: cathodic deposition,[2] simple immersion,[3] and corrosion inhibitors.[4] In recent years, it has been extensively developed to use corrosion inhibitors as an effective method to prevent mild steel against corrosion. For decades, chromate and phosphate-based inhibitors were widely used to protect metals against this massive problem.[5,6] In chromium-based coatings, protection is provided by two oxidation states of Cr; first, the Cr^{3+} oxide offers barrier protection on the metal surface, and second, the Cr^{6+} species provide self-repairing capabilities.[7] Unfortunately, the use of chromate inhibitors is restricted due to their high toxicity and human health effect.[8] For these reasons, the need to research novel corrosion inhibitor compounds has become an essential interest.[9,10] Generally, the presence of inhibitors allows for forming a thin passive film on the metal surface, and consequently reduces corrosive attack.[11,12] Recently, researchers are heading to use less toxic and eco-friendly elements. Rare-earth metal salts, mainly cerium salts can be one of the more viable

alternatives to replace chromate-based compounds. The presence of cerium allows for hindering cathodic oxygen reduction reaction by the formation of a thin layer, which consists of cerium oxide/hydroxide on the metal surface.[13] In aerated solutions, thin oxide films formed are controlled by the reduction of dissolved oxygen to generate OH^- ions (Reaction 1), which increase the pH locally. The pH increase favors the precipitation of cerium hydroxide (Reactions 2–4), resulting in the formation of cerium oxide as the final product (Reaction 5).[14]

$$O_2 + 2H_2O + 4e^- \rightarrow 4OH^-, \quad (1)$$

$$Ce^{3+} + 2OH^- \rightarrow Ce(OH)_2^+, \quad (2)$$

$$Ce^{3+} + 3OH^- \rightarrow Ce(OH)_3 \downarrow, \quad (3)$$

$$4Ce(OH)_3 + O_2 + 2H_2O \rightarrow 4Ce(OH)_4, \quad (4)$$

$$Ce(OH)_4 \rightarrow CeO_2 + 2H_2O. \quad (5)$$

Over the last few years, a variety of inorganic precursors and polymers containing cerium nitrate have been developed to improve the stability of the protective layer.[15] Polyethylene glycol (PEG) is considered an appropriate candidate for corrosion protection of steel, due to its biocompatibility.[16] Mizanur Rahman et al.[17] have synthesized water-borne polyurethane (WBPU)/cerium nitrate dispersions as a green coating on mild steel. The presence of poly tetramethylene oxide (PTMC) considerably increased the barrier effect of a protective coating against corrosion.[17] Furthermore, the addition of the PEG into hybride films obtained by a dip-coating process from a sol that consisted of two alkoxide precursors, 3-(trimethoxysilylpropyl) methacrylate (TMSM) and tetraethoxysilane (TEOS), with 0.01 M of nitrate cerium. The electrochemical results showed that the films improved the corrosion resistance behavior with PEG. Thus, the mechanical results indicated that higher PEG concentrations allowed to give more enhanced durability to the films.[18] In addition, the introduction of PEG in the solution allowed its adsorption by blocking the anodic dissolution reaction at the surface of the steel.[19] In our previous work, the combined effects of cerium nitrate and PEG increased corrosion resistance and decreased the cracked film on the mild steel surface in chloride media.[14] This inspired us to extend further this study to sulfate media. Therefore, the main objective of the present work is to evaluate the inhibition corrosion resistance and elucidate the mechanism of the corrosion inhibition, using $Ce(NO_3)_3$/PEG systems on mild steel in 0.1 M Na_2SO_4 solution.

2 | EXPERIMENTAL METHOD

2.1 | Materials

The substrate tested in this work was prepared from mild steel (ASTM A915) disk; its chemical composition is shown in Table 1.

The samples used in this work were cut from a bar with a diameter of 1.1 cm, then connected to a copper wire. The electrode was embedded in epoxy resin leaving one side 0.95 cm^2 exposed to face the test solution and serving as the working electrode. Subsequently, the finer grades of emery paper were used to abrade each sample's surface until SiC#4000, then, the specimens were washed with distilled water, degreased with ethanol, rinsed again with distilled water to remove ethanol residues, dried with hot air and finally subjected to the experimental tests.

2.2 | Test solutions

The corrosion tests were carried out in analytical grade sodium sulfate (0.1 M Na_2SO_4) solutions (pH = 7.1 and $\sigma = 55.6\ \mu S\ cm^{-1}$) at room temperature (about 25°C) and open to the air. The solutions were gently stirred to obtain a slight vortex of the electrolyte. The inhibiting effect was obtained by dissolving the inhibitors in the corrosive medium. The concentration of cerium nitrate, $Ce(NO_3)_3{,}6H_2O$ (Sigma-Aldrich, $Mw = 434.22$; 99.9%) was increased until 1500 $mg.L^{-1}$, while a fixed concentration of PEG (Sigma-Aldrich, $Mw = 1500$ g/mol) of 2.5 $g.L^{-1}$ [3] was combined with the optimal concentration of cerium nitrate. As a matter of fact, adding PEG with cerium nitrate to 0.1 M Na_2SO_4 could reduce both pH and conductivity levels of the solution (from pH = 5.75 to 5.60 with PEG, and from $\sigma = 17.33$ to 16.39 $\mu S.\ cm^{-1}$).

2.3 | Immersion tests and electrochemical corrosion evolution

The electrochemical measurements were performed using a PGZ 301 (Voltalab 40 model) potentiostat/galvanostat coupled to a frequency response analyzer

TABLE 1 Nominal composition of ASTM A915 mild steel (in wt.%).

C	Si	Mn	S	Cr	P	Al	V	Sn	Mo
0.33	0.24	0.65	0.024	1.06	0.017	0.007	0.022	0.001	0.015

W	Ni	Cu	Co	Ti	Nb	B	Ta	Fe
0.256	0.003	0.088	0.001	0.001	0.003	0.002	0.014	rest

(FRA) Volta Master IV software. The test system consisted of a classic three electrodes cell, in which a saturated calomel electrode (SCE, 0.24 V vs. NHS), a platinum wire (CE), and a mild steel sample were used as reference, counter, and working electrodes, respectively. The immersion tests were carried out from 30 min to 30 days in a corrosive medium. The potentiodynamic polarization curves were obtained by using a sweep rate of 0.5 mV.s^{-1} (or 30 mV. min^{-1}) between ±250 mV compared to the corrosion potential (E_{corr}). The linear polarization resistance measurements (LPR) were obtained between ±20 mV/E_{corr}, and at 0.167 mV.s^{-1} of scan rate. The impedance data were obtained at the corrosion potential (E_{corr}) with an amplitude of 4 mV over the frequency range 100 kHz–5 mHz. The EIS response from the samples was fitted using ZView software. All the corrosion tests were performed between two and three times for reproducibility purposes.

2.4 | Surface characterization of the films

The morphology of the films formed on mild steel was analyzed by a field emission environmental scanning electron microscope (FE-SEM) of FEI Quanta 200 F coupled to an X-ray energy dispersive spectroscopy (EDS) using an EDAX detector to study the local composition of films. The Raman spectra were recorded using a Jobin-Yvon LabRam HR8000 spectrometer equipped with a confocal microscope using an incident monochromatic beam of 632.82 nm emitted by a He–Ne laser. The Raman essays were carried out in the wavenumber range from 200 to 1500 cm^{-1}.

3 | RESULTS AND DISCUSSION

3.1 | Effect of cerium nitrate inhibitor and PEG addition

3.1.1 | Polarization and electrochemical impedance behavior

Polarization behavior

Figure 1a shows the potentiodynamic polarization curves of the mild steel immersed in 0.1 M Na_2SO_4 solution containing various concentrations of cerium nitrate, obtained after 30 min of immersion time at room temperature. The electrochemical parameters such as E_{corr}, I_{corr}, Rp, and IE (corrosion potential, corrosion current density, polarization resistance, and inhibition efficiency, respectively), are collected in Table 2. These corrosion parameters were calculated using the Stern-Geary method: $I_{corr} = \frac{\beta a}{2.3\ Rp}$, or/ and $I_{corr} = \frac{1}{2.3\ Rp}\frac{(\beta a.\beta c)}{(\beta a+\beta c)}$ (the first equation was utilized where the mild steel was under cathodic control, while the second one was applied mainly for free mild steel)[20]; where βa and βc are the anodic and cathodic Tafel slopes, respectively. The inhibition efficiency (IE %) was calculated using the following equation: IE (%) = 100 × ($I^{\circ}_{corr} - I_{corr}$)/$I^{0}_{corr}$, where I^{0}_{corr} and I_{corr} present corrosion current density values for uninhibited (blank) and inhibited substrates, respectively.

In the presence of cerium nitrate inhibitor, the corrosion potential (E_{corr}) is slightly shifted to the negative direction, compared to bare mild steel. Thus, the increase of inhibitor concentration (from 100 to 1500 mg.L^{-1}) allowed to move the E_{corr} toward more

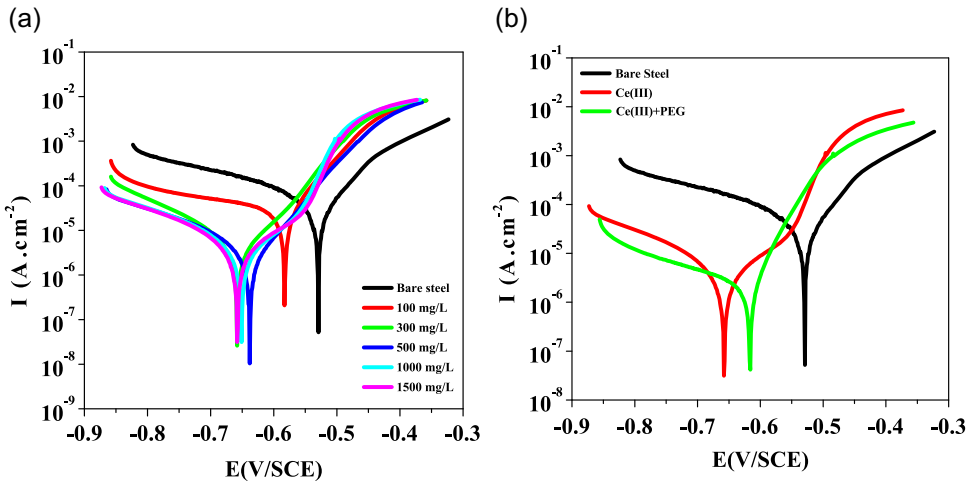

FIGURE 1 Potentiodynamic polarization curves for mild steel in 0.1 M Na_2SO_4 solution at room temperature (a) with increasing concentration of cerium nitrate inhibitor and (b) with 2.5 g.L^{-1} polyethylene glycol (PEG) addition for 30 min of immersion time. [Color figure can be viewed at wileyonlinelibrary.com]

TABLE 2 Electrochemical parameters calculated from polarization measurements on the mild steel electrode in 0.1 M Na_2SO_4 solution with and without various concentrations of cerium nitrate, and with 2.5 $g.L^{-1}$ polyethylene glycol (PEG) addition, at room temperature.

Concentration (mg/L)	E_{corr} (mV/SCE)	βa (mV/dec)	βc (mV)	Rp (Ω. cm²)	I_{corr} (μA/cm²)	IE (%)
Blank	−531	94.2	283.7	204	150.10	-
100	−582	77.8	372.4	490	57.10	61.95
300	−654	66.3	112.7	824	22.02	85.32
500	−638	67.1	147.7	1981	10.12	93.25
1000	−651	52.5	205.8	2061	08.82	94.12
1500	−656	49.6	202.6	2511	06.90	95.40
Ce + PEG	−616	66.0	470.0	4266	05.89	96.07

negative values, with a decrease of the cathodic branches, indicating that the cerium nitrate acts as a cathodic inhibitor in sulfated media. The change in the kinetics of oxygen reaction reduction is due to the blockage effect of Ce^{3+} salts on the cathodic sites through the precipitation of cerium hydroxide/oxide film on the surface.[21] The inhibition efficiency values (IE) are presented in Table 2, which shows that the inhibition efficiency value increases with increasing of cerium nitrate concentration. In addition, the corrosion current density (I_{corr}) reduced and polarization resistance (Rp) rose. The highest protection efficiency value is obtained at 1500 $mg.L^{-1}$ concentration of cerium nitrate (IE = 95.40%), indicating that the active sites on the mild steel surface have all become saturated, each site by at least a single particle of Ce^{3+}. Generally, it is known that the optimal concentration of an inhibitor depends on some parameters, such as the following: metal, type of inhibitor, corrosive medium, temperature, and pH of the solution.[22] Moreover, with PEG addition (Figure 1b), it is observed that the corrosion potential (E_{corr}) has undergone a shift toward more noble potentials, compared to that obtained without PEG addition. It is clearly seen the reduction in the current densities of the anodic and cathodic branches (see Figure 1b), indicates that PEG is allowed to block the anodic reaction and make the films obtained from cerium nitrate inhibitor in the cathodic part more stable. Therefore, PEG appears to form a physical barrier preventing both dissolution and reduction reactions (mixed inhibitor), with a major predominance of anodic control. A relative increase in inhibition efficiency of about 1% was also noted with the addition of PEG (IE = 96.07%). In addition, it is clear from Figure 1b, that the Ce^{3+}/PEG system acted as a mixed inhibitor with a dominant effect on the cathodic part.

Electrochemical impedance spectroscopy (EIS)

The Nyquist and Bode plots (EIS diagrams) of mild steel electrodes obtained after 30 min of immersion time in 0.1 M Na_2SO_4 solution without ("bare steel"), with different amounts of cerium nitrate and with 2.5 $g.L^{-1}$ PEG addition, are shown in (Figure 2a–c). The results of the EIS data fitted with the Zview software are reported in Table 3. For obtaining a good fitting of our EIS spectra, the error factor (χ^2) was limited to a value lower than 0.002, which indicates the suitability of the used equivalent circuit model. As shown in Figure 3, the electrical equivalent circuits are proposed for modeling EIS data. In these circuit models, R_s, R_c, and R_{ct} represent the solution resistance, the outer porous coating resistance, and the charge transfer resistance at the interface, respectively. Thus, the constant phase elements CPE_c and CPE_{dl} are the nonideal (dispersive) layer capacitance and double-layer capacitance respectively. Also, the n values represent a nonlinear coefficient; this value is varied between 0 and 1. The value $n = 1$ is given when CPE is a pure capacitive C; when $n = 0.5$, it corresponds to the diffusion phenomena or a porous material, and when $0.5 < n < 1$, it represents the heterogeneity of the sample surface.[18] Moreover, the inductive elements L and R_L are, respectively, the inductance and its corresponding resistance indicating EIS data of the inductive loop. The equivalent circuit model presented in Figure 3a is proposed for the electrochemical behavior of EIS data of tests gotten without inhibitor (blank), and with cerium nitrate inhibitor concentrations varying from 100 to 300 $mg.L^{-1}$. However, another model exposed in Figure 3b is proposed for EIS data obtained for mild steel containing various concentrations of cerium nitrate inhibitor from 500 to 1500 $mg.L^{-1}$ and with PEG addition, where the shape of the Nyquist plot is very similar to that of the plot obtained with 1500 $mg.L^{-1}$ of cerium inhibitor. The EIS diagrams for bare mild steel in Na_2SO_4 solution (Figure 2a,b) exhibit two time constants at high frequencies (HF) and middle frequencies (MF) that

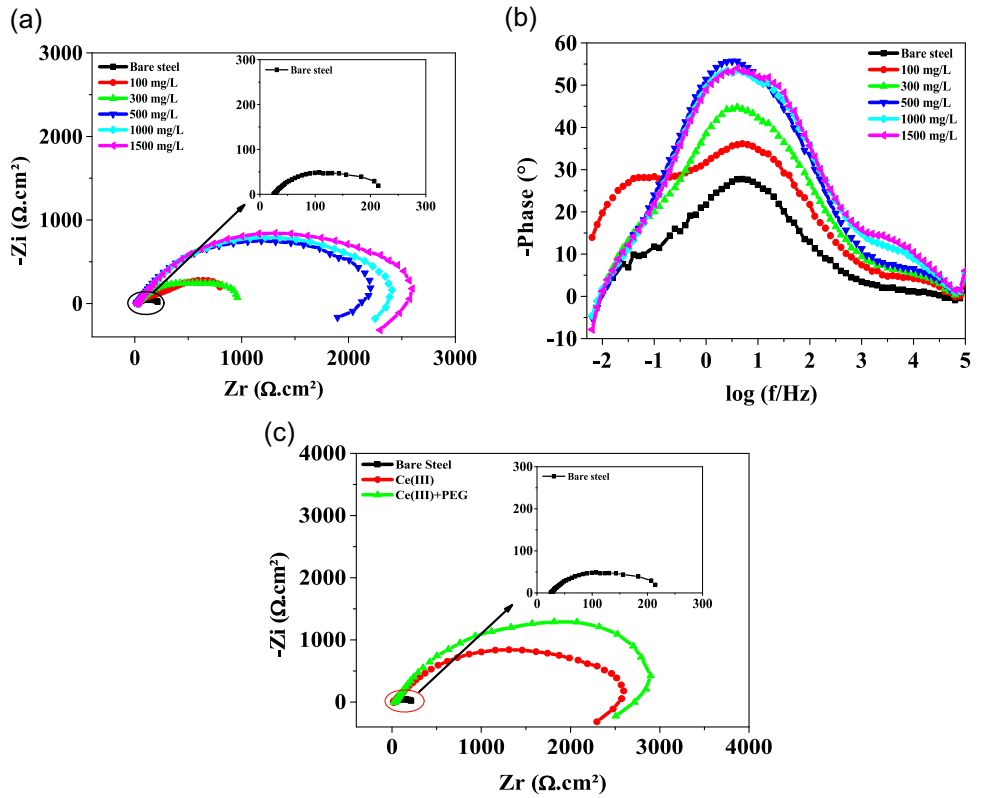

FIGURE 2 Nyquist and Bode diagrams obtained for mild steel in 0.1 M Na_2SO_4 solution at room temperature, (a, b) with increasing concentration of cerium nitrate inhibitor, (c) with polyethylene glycol (PEG) addition, for 30 min of immersion time. [Color figure can be viewed at wileyonlinelibrary.com]

TABLE 3 Fitting results for the electrochemical impedance spectroscopy (EIS) data of mild steel electrode without inhibitor (bare), with cerium nitrate inhibitor and with 2.5 $g.L^{-1}$ polyethylene glycol (PEG) addition after 30 min of immersion in 0.1 M Na_2SO_4 solution and at room temperature.

Concentration mg/L	R_s Ω cm^2	n_c	CPE_c μF cm^{-2} $s^{(n-1)}$	R_c Ω cm^2	n_{dl}	CPE_{dl} μF cm^{-2} $s^{(n-1)}$	R_{ct} Ω cm^2	L (H)	R_L Ω cm^2
Blank	29.37	0.63	161.43	165.60	0.60	283.44	74.0		
100	20.54	0.57	150.54	469.00	0.82	73.70	604	0.033	445
300	19.07	0.79	25.28	144.90	0.65	71.08	877	0.253	280
500	18.57	0.73	46.42	652.00	0.72	33.96	1374	0.862	294
1000	16.73	0.73	49.40	1069.00	0.71	42.43	1420	0.303	428
1500	17.03	0.76	33.45	1330.00	0.71	26.23	1690		
Ce + PEG	20.03	0.75	13.66	1289.00	0.75	24.97	1800		

appeared to be a single capacitive loop. In the HF range, there is a one-time constant that may be due to corrosion products accumulated from the corrosion mechanism of the metal surface, while there is another one in the MF range that can be attributed to the charge transfer processes at the metal/solution interface.[23,24] As the cerium nitrate inhibitor concentration increases up to 1500 $mg.L^{-1}$ (Figure 2a), it is observed an increase in the diameter of Nyquist plots, indicating the increase in corrosion resistance of the substrate. Indeed, the shape of Nyquist and Bode plots remains similar for 100 and 300 $mg.L^{-1}$ of cerium concentration to that obtained without inhibitor (bare). However, by increasing the inhibitor concentration up to 500 $mg.L^{-1}$, the shape of the obtained diagrams began to be different. With the presence of cerium nitrate inhibitor and PEG addition, it is apparent from the EIS diagrams that the

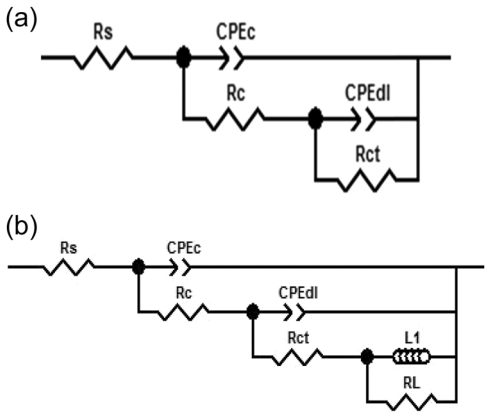

FIGURE 3 Equivalent circuits model representing the interface used to fit the experimental electrochemical impedance spectroscopy (EIS) data of electrodes without (bare), containing various concentrations of cerium nitrate and with 2.5 $g.L^{-1}$ polyethylene glycol (PEG) addition after 30 min of immersion in 0.1 M Na_2SO_4.

capacitive loop is flattened, characterized by two uncoupled relaxation times. At HFs, the first one is observed and can be explained by the formation of a protective film composed of a porous outer layer of cerium hydroxide and a more compact inner layer of cerium oxide, and the second one, which is observed in the MFs, is associated with the charge transfer resistance.[23,24] The presence of 500, 1000, and 1500 $mg.L^{-1}$ of cerium nitrate concentrations and PEG addition allowed the appearance of a well-observed inductive loop at low frequencies (LF) (see Figure 2a–c). There are several explanations for the inductive behavior, including the relaxation process caused by the adsorption of intermediate species such as SO_4^{2-} on the metal surface, formation of passive films, or redox activities.[25–27] In addition, PEG makes the Nyquist semicircle much larger than it would be without it (Figure 2c), which indicates that PEG has provided more corrosion protection for mild steel in 0.1 M Na_2SO_4 solution. Table 3 shows a continuous increase of R_{ct} and decrease of CPE_{dl} values with increasing cerium nitrate concentration and PEG addition. As a result, the film that protects the metal from corrosion has become more stable due to PEG's presence.

3.1.2 | Morphology and characterization of the films

SEM/EDS

The SEM images and EDS spectra of the analyzed specimens immersed for 30 min in 0.1 M Na_2SO_4 solution (a, b), with 1500 $mg.L^{-1}$ of $Ce(NO_3)_3$ (c, d) and with PEG addition (e, f) are shown in Figure 4. The amounts of S and Ce (at.%) of each film are collected in Table 4. The surface of the specimen obtained in 0.1 M Na_2SO_4 (Figure 4a) is covered with corrosion products; this indicates deterioration of the steel surface. In contrast, with 1500 $mg.L^{-1}$ of cerium nitrate inhibitor (Figure 4c), as observed, there are some cracks scattered here and there through the film, which seems relatively homogeneous and covers the entire surface of mild steel. As a result of shear stresses between the film and substrate, the film cracks.[28] After the addition of 2.5 $g.L^{-1}$ PEG (Figure 4e), the surface becomes extremely homogeneous and crack-free while the worm-like features develop, which indicates the adsorption/deposition of cerium derivatives on the PEG molecules adsorbed on the steel surface.[29] Due to the reduction in film thickness and the diminution of internal stresses created by the release of hydrogen protons (H^+) and the oxygen reduction reaction, this film appears to be less cracked.[15,30] The SEM images obtained when PEG is added do not clearly reveal any sign of corrosion. Moreover, the PEG addition decreases the amount of S in the film and contrariwise, the amount of Ce increases (Table 4). These results confirm the good barrier effect of the film against corrosion obtained with PEG addition.

Raman spectroscopy

In Figure 5, Raman spectra of mild steel surface after 30 min of immersion time in 0.1 M Na_2SO_4 solution, for bare steel, with 1500 $mg.L^{-1}$ cerium inhibitor and with the extra addition of 2.5 $g.L^{-1}$ PEG are shown. The Raman peaks at 220, 286, and 401 cm^{-1} characterize hematite (α-Fe_2O_3), and the bands at about 601, 652, and 1293 cm^{-1} correspond to magnetite (Fe_3O_4), maghemite (γ-Fe_2O_3) and lepidocrocite (γ-FeOOH), respectively.[31–33] There is only one peak at 489 cm^{-1} that can be attributed to goethite (α-FeOOH).[34] Furthermore, the presence of cerium nitrate inhibitor highlights the presence of an intense peak located at about 459 cm^{-1}, attributed to the symmetrical vibration mode of Ce-O[14]; this band was also observed at 449 cm^{-1} by Hamlaoui et al. in the ceria coatings grown by cathodic electrodeposition on low carbon steel.[35] Observations of this band were also made on aluminum and tin metals at 453 and 457 cm^{-1}, respectively.[36] The presence of cerium (Ce) in the film is confirmed by EDS analysis (Figure 4d and Table 4). In addition, the peak at 250 cm^{-1} was attributed to hematite.[37] The Raman vibrations at 379, 645, and 1304 cm^{-1}, and at 530 cm^{-1} were, respectively, attributed to the lepidocrocite and magnetite. In addition, traces of macknawite at around 215 and 302 cm^{-1} and of iron sulfate at 988 cm^{-1} are also observed.[33,38–40] With PEG, the corrosion products related to lepidocrocite (652 and 1293 cm^{-1}), mackinawite (211 cm^{-1}), hematite (241 cm^{-1}), and magnetite (530 cm^{-1}) disappeared and only the iron sulfate peak (988 cm^{-1}) remains. In contrast, the peak of CeO_2 (459 cm^{-1}) is very intense, which indicates that the mild steel substrate is quite protected with the combination of 1500 $mg.L^{-1}$ of $Ce(NO_3)_3$ and 2.5 $g.L^{-1}$ of PEG.

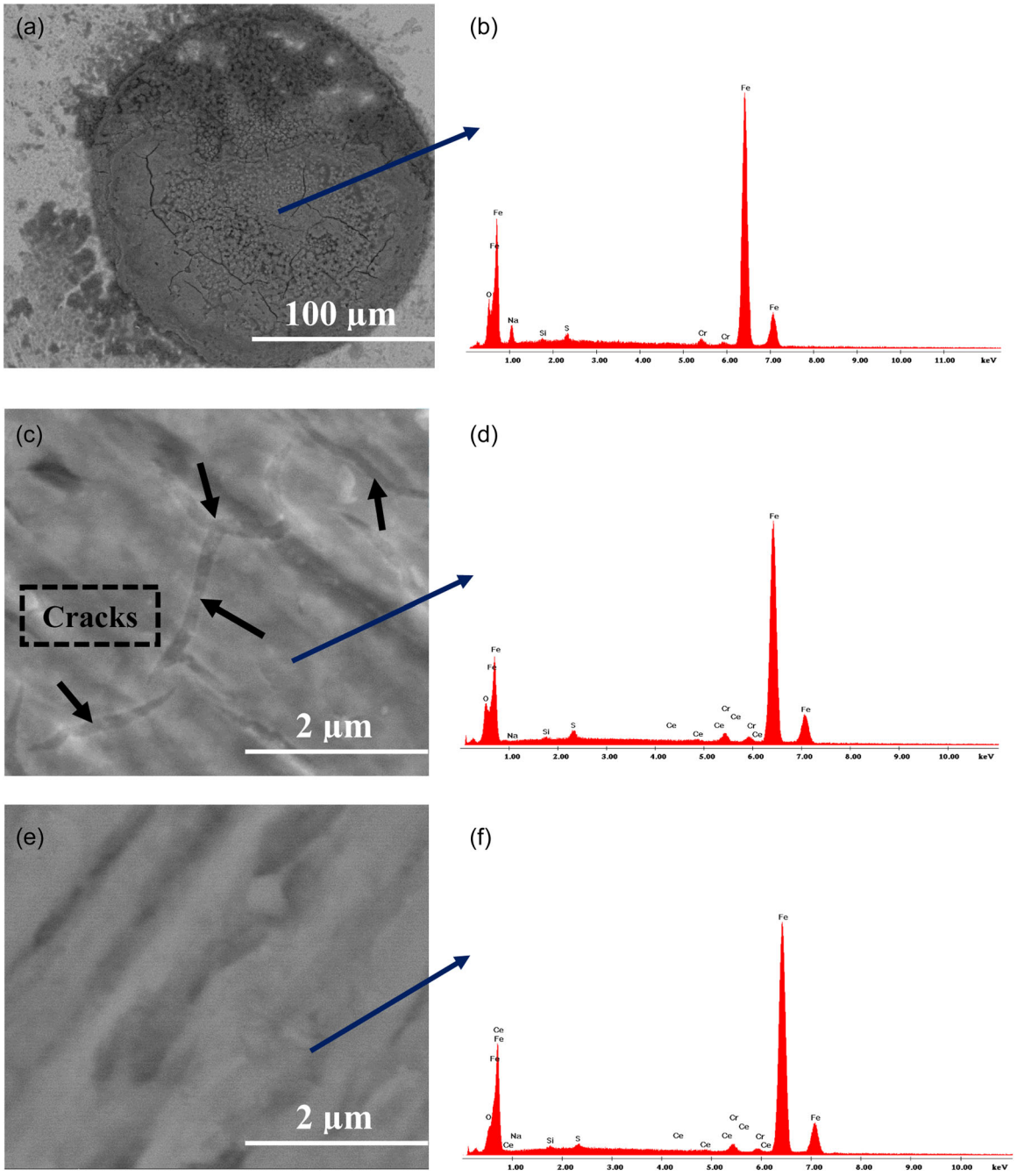

FIGURE 4 SEM images and energy dispersive spectroscopy (EDS) spectra of mild steel surface obtained after 30 min of immersion in 0.1 M Na_2SO_4 solution: (a, b) bare steel, (c, d) with the presence of 1500 mg.L^{-1} cerium nitrate inhibitor and (e, f) with 2.5 g.L^{-1} polyethylene glycol (PEG) addition. [Color figure can be viewed at wileyonlinelibrary.com]

TABLE 4 Sulfur (S) and cerium (Ce) (at.%) contents in the film retrieved by energy dispersive spectroscopy (EDS) after 30 min of immersion at room temperature in 0.1 M Na_2SO_4: bare mild steel, with 1500 mg.L^{-1} cerium inhibitor and with the extra addition of 2.5 g.L^{-1} polyethylene glycol (PEG).

	S (at.%)	Ce (at.%)
Bare mild steel	1.10	-
Ce	0.51	0.22
Ce + PEG	0.45	0.25

3.2 | Effect of immersion time

3.2.1 | Polarization and electrochemical impedance behavior

The effect of exposure time on the corrosion inhibition in 0.1 M Na_2SO_4 solution with 1500 mg.L^{-1} cerium inhibitor and with the extra addition of 2.5 g.L^{-1} PEG was investigated by using potentiodynamic techniques. For simplification of the text, in this paper, only the

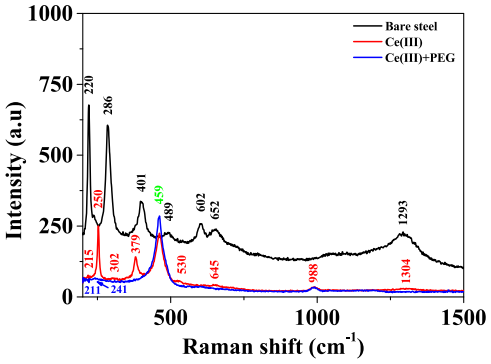

FIGURE 5 Raman spectra of mild steel surface obtained after 30 min of immersion in 0.1 M Na_2SO_4 at room temperature for bare steel and with 1500 mg.L^{-1} cerium inhibitor and with 2.5 g.L^{-1} polyethylene glycol (PEG) addition.

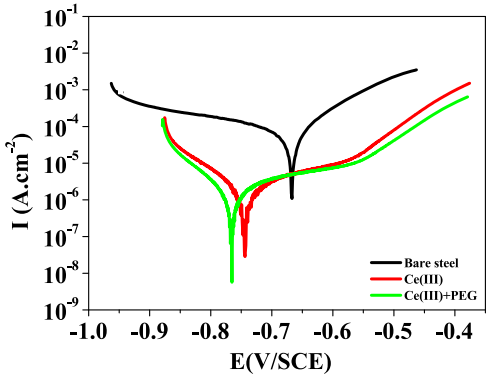

FIGURE 6 Potentiodynamic polarization curves for mild steel recorded in 0.1 M Na_2SO_4 solution with 1500 mg.L^{-1} cerium inhibitor and with the extra addition of 2.5 g.L^{-1} polyethylene glycol (PEG) for 30 days of immersion time. [Color figure can be viewed at wileyonlinelibrary.com]

polarization curves obtained after just 30 days of immersion time are presented (Figure 6), while Table 5 gathers the full electrochemical parameters deduced from 30 min until 30 days of immersion time for bare, with cerium nitrate and with PEG. Compared to untreated samples, both treatments shift the corrosion potential to more cathodic values, which is due to the formation of a protective layer onto the surface of the substrate. Moreover, it seems that the evolution of the current densities with immersion time in both cases followed the same trend (Figure 7), but PEG reduced slightly the corrosion current density (I_{corr}) of the substrate, which indicates the formation of a more protective layer. Thus, the inhibition efficiency (IE %) remains almost stable at around 99% throughout the soak time.

Figure 6 illustrates the potentiodynamic curves of the substrate in 0.1 M Na_2SO_4 solution, with (Ce) and (Ce + PEG), after 30 days of immersion, where it is observed a decrease in the current densities of both anodic and cathodic branches provided by PEG addition, indicating that the PEG enhanced the stability of the film and suppressed metal dissolution during the anodic reaction.

Figure 8a,b displays the evolution of Nyquist and Bode plots, during immersion time up to 30 days of a steel electrode (blank) in 0.1 M Na_2SO_4 solution. It is evident from the general shape of these curves that there are two uncoupled relaxation times at high and middle frequencies. The first one characterizes the resistance of the corrosion products film (R_c), and the second one represents the charge transfer resistance (R_{ct}).[41] It should be noted here that from the first day of immersion, the phenomenon of diffusion (resistance diffusion) at low frequencies is observed, characterized by the diffusion of oxygen and reactive species at the interface (metal/solution). Therefore, the equivalent circuit was revised to include a resistance diffusion (W). The general equivalent electrical circuit proposed for modeling these EIS curves is presented in Figure 8a. The values of the parameters W_{1R}, W_{1T}, and W_{1P} obtained from the fitted results, which indicate, respectively, the diffusion resistance, diffusion capacitive, and diffusion of nonlinear coefficient are listed in Table 6. A decrease of the transfer resistance (R_{ct}) occurs with increasing immersion time up to 10 days and then, the R_{ct} increases, which indicates the formation of a passive film at the surface of the substrate. The Bode diagrams between 10 and 30 days display a clear increase of the phase angle values at low frequencies with increasing immersion time, which can be associated with a decrease in the corrosion rate with time. Moreover, at middle frequencies, the max angle phase declines with immersion time and shifts toward low frequencies indicating a substantial reduction of the capacitive behavior.

Figure 8c–f shows the EIS diagrams (Nyquist and Bode) with 1500 mg.L^{-1} cerium inhibitor and with the extra addition of 2.5 g.L^{-1} PEG. The spectra consist of two uncoupled relaxation times, which represent the film and charge transfer resistance at high and middle/low frequencies (HF and M-LF) (an equivalent circuit is proposed in Figure 8c,e, for modeling the impedance data—Table 6). In general, both treatments improve the corrosion resistance of the substrate indicated by the initial impedance recorded 30 min after electrode immersion. Moreover, the R_{ct} values of the deposits obtained with PEG addition are greater than those obtained only with cerium nitrate inhibitor during the most period of immersion. It is also noted that the initial impedance drifts but not continuously toward an increasing value with immersion time. A nonuniform evolution of R_{ct} values is due mainly to penetration of the aggressive

TABLE 5 Electrochemical parameters of bare mild steel metal with 1500 mg.L^{-1} cerium inhibitor and with the extra addition of 2.5 g.L^{-1} polyethylene glycol (PEG) inhibitors at different immersion times in 0.1 M Na_2SO_4 solution.

Sample	Immersion time	E_{corr} (mV/SCE)	βa (mV/dec)	βc (mV)	I_{corr} (μA/cm²)	EI (%)
Bare mild steel	30 min	−531	94.2	283.7	150.72	-
	2 h	−551	93.2	184.9	288.70	-
	8 h	−585	129.0	160.0	320.28	-
	1 day	−634	189.9	169.7	416.94	-
	3 days	−633	183.4	173.3	372.22	-
	5 days	−656	179.4	162.4	523.15	-
	10 days	−659	136.1	175.2	392.30	-
	20 days	−662	127.9	189.2	409.36	-
	30 days	−677	122.5	189.5	439.10	-
Ce	30 min	−656	49.6	202.6	06.90	95.40
	1 day	−707	185.5	150.3	07.03	98.31
	3 days	−735	167.1	240.8	06.33	98.29
	5 days	−722	148.3	123.8	04.74	99.09
	10 days	−718	163.3	128.9	06.67	98.29
	20 days	−632	74.7	147.5	10.95	97.32
	30 days	−744	193.2	80.6	05.58	98.72
Ce + PEG	30 min	−616	66.0	470.0	05.89	96.07
	1 day	−675	91.3	143.4	4.07	99.02
	3 days	−704	70.2	105.3	1.89	99.49
	5 days	−701	110.7	126.7	3.56	99.32
	10 days	−703	74.5	104.4	3.13	99.20
	20 days	−754	188.7	98.1	5.32	98.70
	30 days	−765	235.1	68.9	4.40	99.00

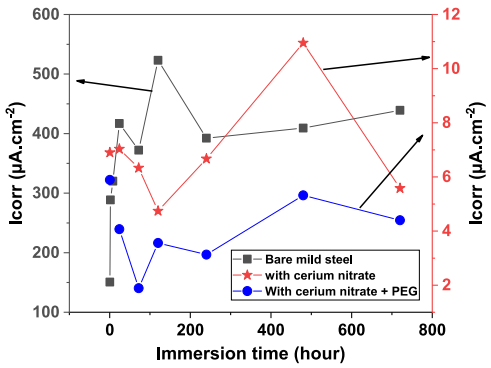

FIGURE 7 Evolution of Icorr as a function of immersion time in 0.1 M Na_2SO_4 solution for bare mild steel, with 1500 mg.L^{-1} cerium inhibitor and with the extra addition of 2.5 g.L^{-1} polyethylene glycol (PEG) until 30 days of immersion. [Color figure can be viewed at wileyonlinelibrary.com]

solution through cracks and defects in the coating inducing a dissolution/passivation state known as self-healing phenomena.[42,43] The presence and the contribution of the coating are also highlighted in the Bode plots where the two-time constants are well distinguished. Moreover, we can easily see a displacement of the max angle phase at MF toward high frequencies. Figure 8g shows Nyquist plots of the mild steel obtained with and without PEG addition in 0.1 M Na_2SO_4 solution after 30 days of immersion time. The R_{ct} of the curve obtained with the presence of PEG seems about three times (Table 6) higher than the one obtained without PEG. Thus, it is observed that the value of CPE_{dl} decreased with PEG, confirming again that the PEG addition attributed to the increase in the resistance of mild steel after 30 days of immersion.

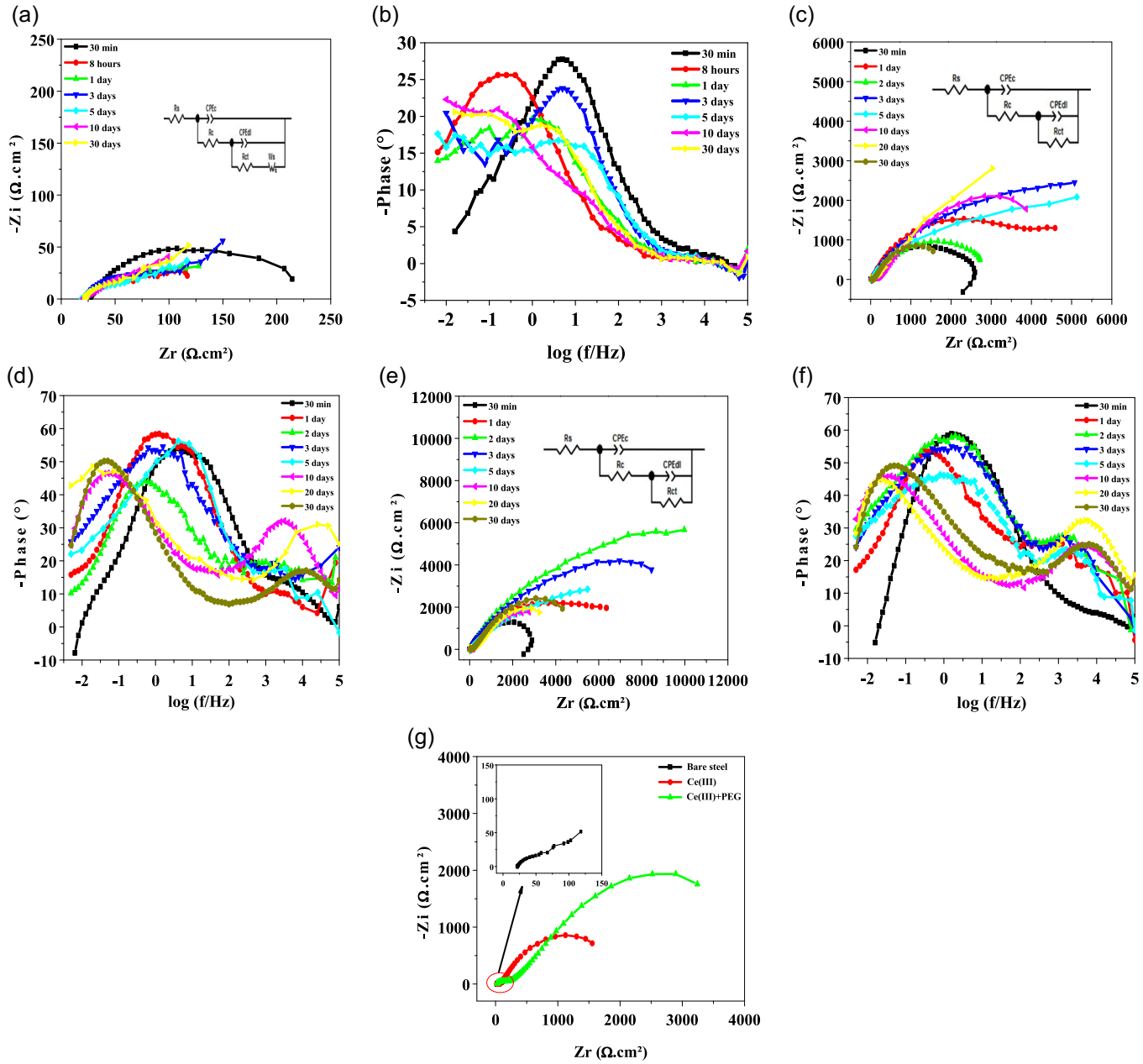

FIGURE 8 Electrochemical impedance spectroscopy (EIS) diagrams (Nyquist & Bode) recorded in 0.1 M Na_2SO_4 solution as a function of immersion time for (a, b) bare mild steel; (c, d) with 1500 mg.L^{-1} cerium inhibitor and (e, f) with the extra addition of 2.5 g.L^{-1} polyethylene glycol (PEG). (g) Compares the Nyquist curves after 30 days of immersion. [Color figure can be viewed at wileyonlinelibrary.com]

3.2.2 | Morphology and characterization of the films

SEM/EDS

Figure 9 shows the morphology of the different films on a mild steel surface after 30 days of immersion in 0.1 M Na_2SO_4 solution (bare, with Ce, and with PEG addition). A general view of Figure 9a reveals that the surface of mild steel is covered with a thick and heterogeneous film of corrosion products. In the presence of Ce (Figure 9b,c), the film becomes thin and compact so that corrosion is inhibited. The film looks homogeneous, but it contains nodules and cracks. In contrast, the addition of PEG (Figure 9e,f) results in a film with fewer cracks and fewer nodules. Moreover, Table 7 displays the amount of Ce (at.%) in the films obtained with the presence of cerium and with PEG addition in 0.1 M Na_2SO_4 solution. The results exhibit that the PEG could increase the amount of

TABLE 6 Fitting results for the electrochemical impedance spectroscopy (EIS) data of bare mild steel metal, with 1500 mg.L^{-1} cerium inhibitor and with the extra addition of 2.5 g.L^{-1} polyethylene glycol (PEG) inhibitors at different immersion times in 0.1 M Na_2SO_4 solution.

Sample	Time	Rs Ω cm^2	n_c	CPE_c μF s$^{(n-1)}$ cm^{-2}	R_c Ω cm^2	n_{dl}	CPE_{dl} μF s$^{(n-1)}$ cm^{-2}	R_{ct} Ω cm^2	$W_{1\text{-}R}$ Ω cm^2	$W_{1\text{-}T}$ Ω^{-1} cm^{-2}	$W_{1\text{-}P}$
Bare mild steel	30 min	29.37	0.63	161.43	165	0.60	283.44	74.00	-	-	-
	8 h	21.40	0.61	738.65	59	0.75	859.16	54.20	-	-	-
	1 day	20.93	0.62	694.11	51	0.63	290.71	50.30	429	1.04	0.34
	3 days	20.44	0.69	280.02	66	0.76	379.26	53.00	319	4.27	0.38
	5 days	19.21	0.63	389.90	38	0.67	323.8	47.00	263	2.74	0.37
	10 days	20.02	0.63	785.16	17	0.65	230.7	73.40	455	7.14	0.26
	30 days	20.68	0.65	661.90	47	0.64	363.39	25.40	499	3.73	0.28
Ce	30 min	17.03	0.76	33.45	1330	0.71	26.23	1690	-	-	-
	1 day	17.62	0.67	40.90	4554	0.72	40.40	2357	-	-	-
	2 days	28.35	0.59	11.89	1454	0.74	52.26	1825	-	-	-
	3 days	21.61	0.58	36.12	5952	0.74	23.74	2700	-	-	-
	5 days	16.72	0.53	29.00	4563	0.90	82.41	2561	-	-	-
	10 days	18.42	0.62	45.22	3510	0.62	12.25	2680	-	-	-
	20 days	16.28	0.35	25.70	7830	0.55	14.74	3278	-	-	-
	30 days	16.48	0.48	15.15	1480	0.70	37.43	700	-	-	-
Ce + PEG	30 min	20.03	0.75	13.66	1289	0.75	24.97	1800	-	-	-
	1 day	25.63	0.57	18.91	5024	0.76	28.96	2298	-	-	-
	2 days	22.55	0.55	23.49	12 151	0.86	08.05	4807	-	-	-
	3 days	23.81	0.53	27.58	9650	0.82	08.49	3200	-	-	-
	5 days	19.98	0.46	48.50	6800	0.77	13.70	2920	-	-	-
	10 days	19.35	0.56	07.09	3350	0.60	19.59	1574	-	-	-
	20 days	17.89	0.59	04.15	3980	0.56	16.33	1745	-	-	-
	30 days	16.26	0.51	13.36	4620	0.62	10.46	2139	-	-	-

Ce, showing that its addition (of PEG) gave the film more corrosion protection after 30 days of immersion.

Raman spectroscopy

The Raman spectra after 30 days of immersion in 0.1 M Na_2SO_4 are gathered in Figure 10. For the bare sample, the spectrum presents peaks at (220 and 250 cm^{-1}) corresponding to hematite, and other peaks at (347 and 379 cm^{-1}), (480 cm^{-1}), (527 cm^{-1}), and (652 cm^{-1}) typical of the lepidocrocite, goethite, magnetite, and maghemite, respectively.[44] The presence of mackinawite ($Fe_{(1+X)}S$) is also observed at around 302 and 347 cm^{-1}. Thomas et al.[45] demonstrated that only the presence of SO_4^{2-} ions leads to the formation of oxidized iron sulfate complex ($FeSO_4$), according to the following reaction:

$$Fe^{2+} + SO_4^{2-} \rightarrow FeSO_4 + 2e^-. \quad (6)$$

This approach has also been confirmed by Rojas et al.,[46] using Pourbaix's diagram for the Fe^{2+}-SO_4^{2-}-H_2O system. Thus, in previous studies, the authors have shown that iron sulfate formed as corrosion products could convert to mackinawite.[38,40,47] The film obtained without PEG (only with Ce^{3+}), mainly consists of the hematite (250 cm^{-1}), mackinawite (217 and 330 cm^{-1}), iron oxyhydroxides (706 cm^{-1}), iron sulfate (988 cm^{-1}), and sulfated green rust (433 and 506 cm^{-1}).[48,49] It also noted the presence of traces of cerium oxide at about 447 cm^{-1}.

According to the Pourbaix (potential-pH) diagram, it is possible to form sulfated green rust, from the oxidation

of iron sulfate by water,[50] depending on the following reaction:

$$5Fe(OH)_2 + Fe^{2+} + SO_4^{2-} + 1/2O_2 + 9H_2O \rightarrow [Fe_2^{(II)}Fe_3^{(III)}(OH)_{12}SO_4.8H_2O]. \quad (7)$$

In contrast, for the film obtained with PEG addition, the chemical composition consists of hematite (250 cm^{-1}), goethite (297 and 391 cm^{-1}), lepidocrocite (1302 cm^{-1}), mackinawite (206 cm^{-1}), iron oxyhydroxides (544 and 706 cm^{-1}), iron sulfate (983 cm^{-1}), and sulfated green rust (433 cm^{-1}), in addition to CeO_2, clearly observed at

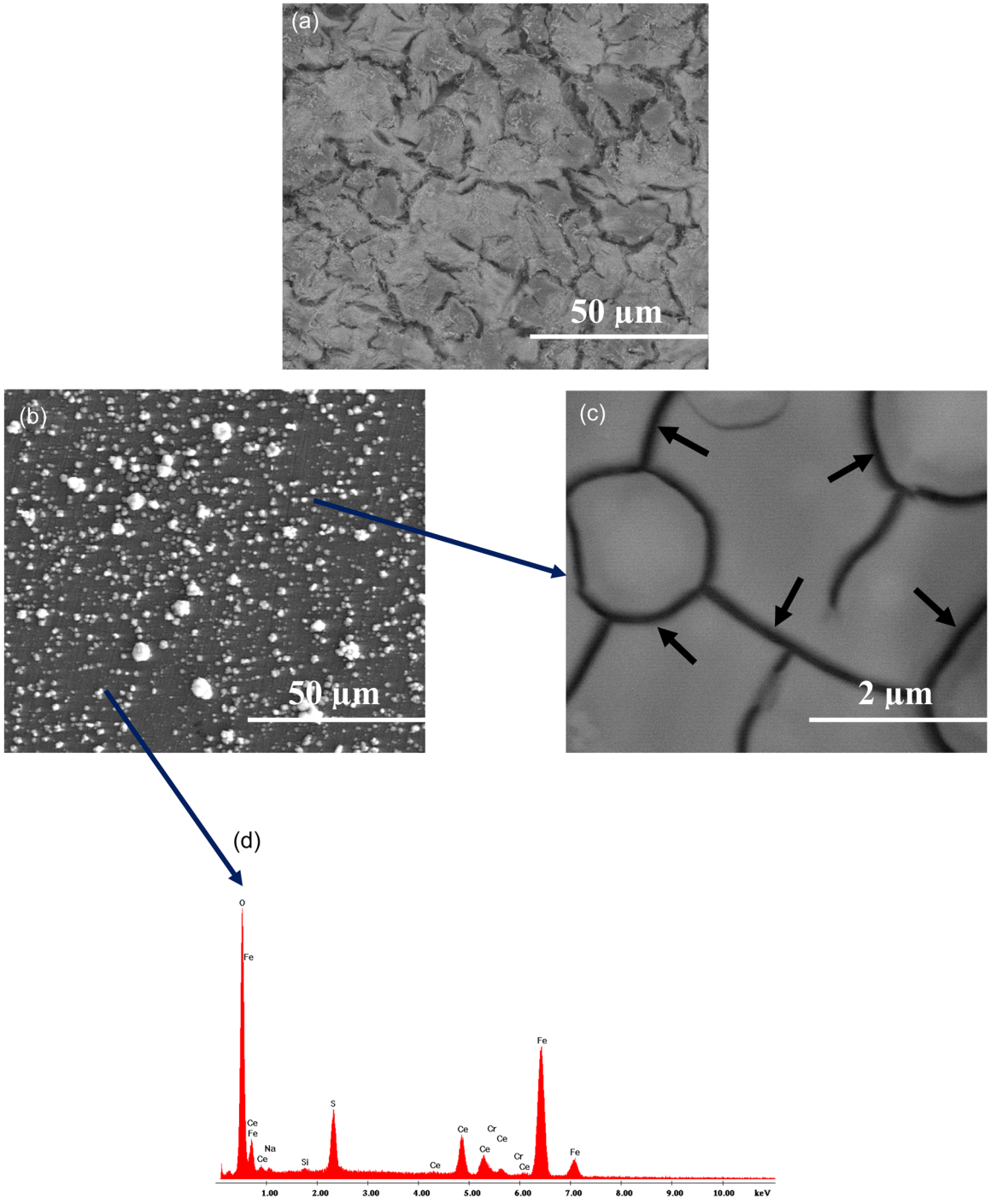

FIGURE 9 SEM morphologies of mild steel surface after 30 days of immersion in 0.1 M Na_2SO_4 solution: (a) bare steel, (b, c) with 1500 $mg.L^{-1}$ cerium inhibitor, and (e, f) with the extra addition of 2.5 $g.L^{-1}$ polyethylene glycol (PEG). (d, g) are the energy dispersive spectroscopy (EDS) spectra obtained with cerium nitrate inhibitor and with PEG addition, respectively. [Color figure can be viewed at wileyonlinelibrary.com]

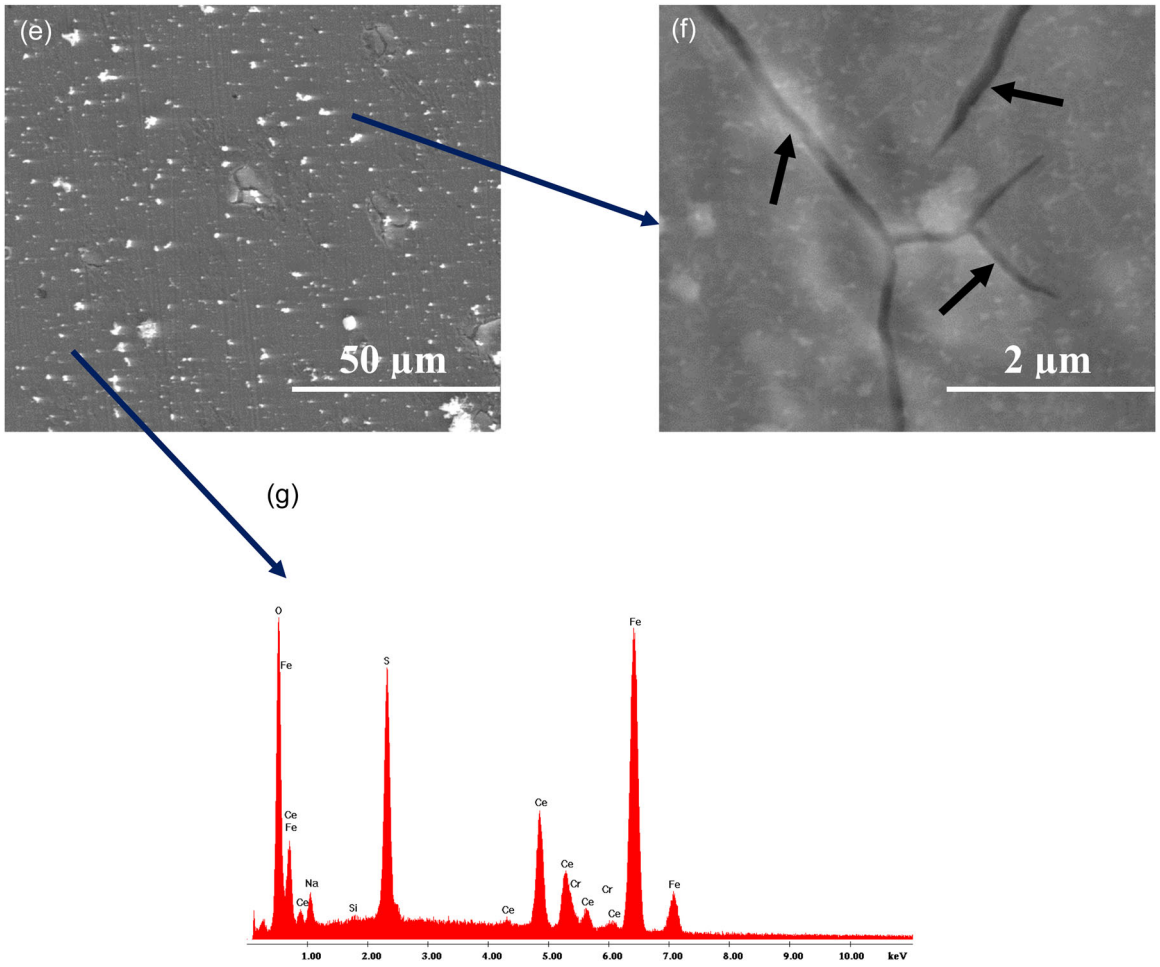

FIGURE 9 (Continued)

TABLE 7 Cerium (Ce) (at.%) content in the film retrieved by energy dispersive spectroscopy (EDS) after 30 days of immersion time and at room temperature in 0.1 M Na_2SO_4 with 1500 mg.L^{-1} cerium inhibitor and with the extra addition of 2.5 g.L^{-1} PEG.

	Ce (at.%)
Ce	4.19
Ce + polyethylene glycol	6.58

447 cm^{-1}. The presence of the lepidocrocite and goethite can be explained here by the transformation of green sulfated rust, first to the lepidocrocite (Reaction 8), which then converts to the goethite (Reaction 9).[31,51,52]

$$[Fe_2^{(II)}Fe_3^{(III)}(OH)_{12}SO_4.8H_2O] + 3/2H_2O_2 \rightarrow 5FeOOH + Fe^{2+} + SO_4^{2-} + 9H_2O, \quad (8)$$

$$\gamma - FeOOH \rightarrow \alpha - FeOOH. \quad (9)$$

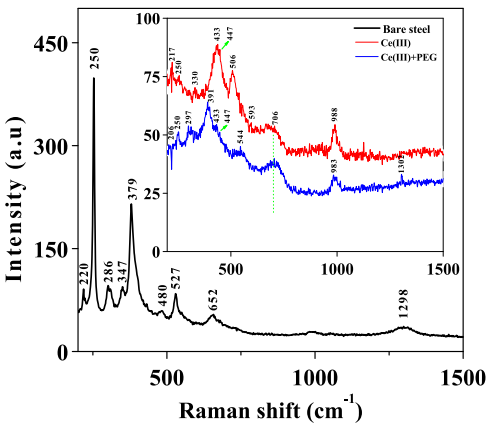

FIGURE 10 Raman spectra of the films obtained after 30 days of immersion at room temperature in 0.1 M Na_2SO_4 solution for bare steel, with 1500 mg.L^{-1} cerium inhibitor and with the extra addition of 2.5 g.L^{-1} polyethylene glycol (PEG). [Color figure can be viewed at wileyonlinelibrary.com]

Here, the presence of goethite contributed to the stability of the film obtained and played a selfprotecting role.[53]

4 | CONCLUSION

In the present work, the corrosion inhibition performance of cerium nitrate and of a combination of cerium nitrate/PEG, was, respectively, studied in 0.1 M Na_2SO_4 solution for ASTM A915 mild steel. The potentiodynamic polarization tests showed that the cerium nitrate acted as a cathodic inhibitor, leading to a slight shift in the corrosion potential to the negative direction. As well, the corrosion resistance of mild steel sharply increased by increasing cerium concentration up to 1500 mg.L^{-1}. Also, a protocol based on EIS results revealed a significant enhancement of R_{ct} and a reduction in CPE_{dl} values when cerium nitrate is present, confirming the inhibition of mild steel against corrosion after a short time immersion. In addition, the PEG addition allowed for increasing relatively the corrosion resistance of mild steel by suppressing the anodic reaction. Moreover, PEG-added film appeared more homogenous; less cracked, and contained fewer nodules.

DATA AVAILABILITY STATEMENT

Data that support the findings of this study are available from the corresponding author upon reasonable request.

ORCID

Hichem Boudellioua http://orcid.org/0000-0003-1089-9956
Youcef Hamlaoui http://orcid.org/0000-0003-0737-7401

REFERENCES

[1] W. D. Callister, *Materials Science and Engineering: An Introduction*, 4th ed., John Willy and Sons, Inc, New York **1997**.
[2] N. Bourenane, Y. Hamlaoui, C. Remazeilles, F. Pedraza, *Mater. Corros.* **2019**, *70*, 110.
[3] H. Boudellioua, Y. Hamlaoui, L. Tifouti, F. Pedraza, *J. Mater. Eng. Perform.* **2017**, *26*, 4402.
[4] D. Dwivedi, K. Lepková, T. Becker, *RSC Adv.* **2017**, *7*, 4580.
[5] J. Sinko, *Prog. Org. Coat.* **2001**, *42*, 267.
[6] A. C. Bastos, M. G. Ferreira, A. M. Simões, *Corros. Sci.* **2006**, *48*, 1500.
[7] X. Zhang, C. van den Bos, W. G. Sloof, A. Hovestad, H. Terryn, J. H. W. de Wit, *Surf. Coat. Technol.* **2005**, *199*, 92.
[8] M. Costa, C. B. Klein, *Crit. Rev. Toxicol.* **2006**, *36*, 155.
[9] C. M. Caruana, C. M. Caruana, *Met. Finish.* **2006**, *104*, 44.
[10] A. Yabuki, Y. Nagayama, I. W. Fathona, *Electrochim. Acta* **2019**, *296*, 662.
[11] C. G. Dariva, A. F. Galio, *Developments in Corrosion Protection*, InTech, Winchester, UK **2014**.
[12] P. Rodič, I. Milošev, M. Lekka, F. Andreatta, L. Fedrizzi, *Electrochim. Acta* **2019**, *308*, 337.
[13] H. Shi, E. H. Han, F. Liu, *Corros. Sci.* **2001**, *53*, 2374.
[14] H. Boudellioua, Y. Hamlaoui, L. Tifouti, F. Pedraza, *Appl. Surf. Sci.* **2019**, *473*, 449.
[15] Y. Hamlaoui, L. Tifouti, F. Pedraza, *J. Mater. Eng. Perform.* **2013**, *22*, 2706.
[16] M. J. Harris, S. Zalipsky, American Chemical Society, Washington, American Chemical Society, Washington **1997**.
[17] M. Rahman, M. Zahir, M. Haq, D. Shehri, A. Kumar, *Coatings*. **2018**, *8*, 34.
[18] S. R. Kunst, H. R. P. Cardoso, L. V. R. Beltrami, C. T. Oliveira, T. L. Menezes, J. Z. Ferreira, C. F. Malfatti, *Mater. Res.* **2015**, *18*, 138.
[19] E. Guilminot, F. Dalard, C. Degrigny, *Corros. Sci.* **2002**, *44*, 2199.
[20] M. Stern, A. L. Geaby, *J. Electrochem. Soc.* **1957**, *104*, 56.
[21] A. Dastgheib, M. Mohammadzadeh Attar, A. Zarebidaki, *Met. Mater. Int.* **2020**, *26*, 1634.
[22] A. Zarrouk, H. Zarrok, R. Salghi, B. Hammouti, F. Bentiss, R. Touir, M. Bouachrine, *J. Mater. Environ. Sci.* **2013**, *4*, 177.
[23] F. Ivušić, O. Lahodny-Šarc, H. O. Ćurković, V. Alar, *Corros. Sci.* **2015**, *98*, 88.
[24] K. Aramaki, *Corros. Sci.* **2001**, *43*, 2201.
[25] M. Gobara, A. Baraka, R. Akid, M. Zorainy, *RSC Adv.* **2020**, *10*, 2227.
[26] P. C. Okafor, C. B. Liu, X. Liu, Y. G. Zheng, *J. Appl. Electrochem.* **2009**, *39*, 2535.
[27] S. A. Salih, A. A. Mazhar, M. H. Mahanny, *Port. Electrochim. Acta* **2004**, *22*, 205.
[28] H. Boudellioua, Y. Hamlaoui, L. Tifouti, F. Pedraza, *Mater. Corros.* **2020**, *71*, 1300.
[29] K. Aramaki, *Corros. Sci.* **2006**, *48*, 766.
[30] Y. Hamlaoui, H. Boudellioua, L. Tifouti, F. Pedraza, *J. Mater. Eng. Perform.* **2015**, *24*, 4626.
[31] X. Zhang, K. Xiao, C. Dong, J. Wu, X. Li, Y. Huang, *Eng. Failure Anal.* **2011**, *18*, 1981.
[32] L. Bellot-Gurelet, D. Neff, S. Réguer, J. Monnier, M. Saheb, P. Dillman, *J. Nano Res.* **2009**, *8*, 147.
[33] G. Genchev, A. Erbe, *J. Electrochem. Soc.* **2016**, *163*, C333.
[34] G. P. Singh, A. P. Moon, S. Sengupta, G. Deo, S. Sangal, K. Mondal, *J. Mater. Eng. Perform.* **2015**, *24*, 1961.
[35] Y. Hamlaoui, F. Pedraza, L. Tifouti, *Corros. Sci.* **2008**, *50*, 2182.
[36] A. Siokou, S. Ntais, V. Dracopoulos, S. Papaefthimiou, G. Leftheriotis, P. Yianoulis, *Thin Solid Films* **2006**, *514*, 87.
[37] D. de la Fuente, J. Alcántara, B. Chico, I. Díaz, J. A. Jiménez, M. Morcillo, *Corros. Sci.* **2016**, *110*, 253.
[38] J. A. Bourdoiseau, M. Jeannin, R. Sabot, C. Rémazeilles, P. Refait, *Corros. Sci.* **2008**, *50*, 3247.
[39] R. Sabot, M. Jeannin, M. Gadouleau, Q. Guo, E. Sicre, P. Refait, *Corros. Sci.* **2007**, *49*, 1610.
[40] B. W. A. Sherar, I. M. Power, P. G. Keech, S. Mitlin, G. Southam, D. W. Shoesmith, *Corros. Sci.* **2011**, *53*, 955.
[41] F. F. Eliyan, E. S. Mahdi, A. Alfantazi, *Corros. Sci.* **2012**, *58*, 181.
[42] Y. Ma, Y. Li, F. Wang, *Corros. Sci.* **2009**, *51*, 997.
[43] J. M. Ferreira, Jr., K. P. Souza, F. M. Queiroz, I. Costa, C. R. Tomachuk, *Surf. Coat. Technol.* **2016**, *294*, 36.
[44] M. Legodi, D. de Waal, *Dyes Pigm.* **2007**, *74*, 161.
[45] J. G. N. Thomas, A. D. Mercer, J. D. Davies, *Proc. Int. Conf. Corros. Inhibit* (Ed: R. H. Heusler), **1983**, 89.

[46] A. Rojas-Hernández, M. T. Ramírez, J. G. Ibáñez, I. González, *J. Electrochem. Soc.* **1991**, *138*, 365.
[47] M. Langumier, R. Sabot, R. Obame-Ndong, M. Jeannin, S. Sablé, P. Refait, *Corros. Sci.* **2009**, *51*, 2694.
[48] P. Refait, M. Abdelmoula, J.-M. R. Génin, *Corros. Sci.* **1998**, *40*, 1547.
[49] M. Abdelmoula, P. Refait, S. H. Drissi, J.-P. Mihe, J.-M. R. Génin, *Corros. Sci.* **1996**, *38*, 623.
[50] M. Jeannin, A. Olowe, P. h Refait, L. Simon, *Corros. Sci.* **1996**, *38*, 1751.
[51] J. Bessiere, M. Perdicakis, B. Humbert. *Comptes Rendus de l'académie Des Sciences*, Série IIC, Chimie, **1999**, 2.
[52] P. Refait, J. B. Memet, C. Bon, R. Sabot, J.-M. R. Génin, *Corros. Sci.* **2003**, *45*, 833.
[53] M. Yamashita, H. Miyuki, Y. Matsuda, H. Nagano, T. Misawa, *Corros. Sci.* **1994**, *36*, 283.

How to cite this article: H. Boudellioua, Y. Hamlaoui, L. Tifouti, F. Pedraza, *Mater. Corros.* **2023**, 1–15. https://doi.org/10.1002/maco.202313727